Remote Sensing of Roads and Highways in Colorado

Large-Area Road-Surface Quality and Land-Cover Classification Using Very-High Spatial Resolution Aerial and Satellite Data

Contract No. **RITARS-12-H-CUB**

Quarterly Progress Report #5

Quarter from 10/01/2013 to 12/31/2013

Principal Investigator
Dr. William Emery
Professor
Aerospace Engineering Science Department,
University of Colorado at Boulder

Program Manager
Mr. Caesar Singh
Research Innovative Technology Administration,
U.S. Department of Transportation

Contents

GLOSSARY

CDOT	Colorado Department of Transportation
CU	University of Colorado
DG	DigitalGlobe
DN	Digital Number
IRI	International Roughness Index
MPO	Municipal Planning Office
PPACG	Pikes Peak Area Council of Government
QB	QuickBird
WV-1	WorldView-1
WV-2	WorldView-2

EXECUTIVE SUMMARY

Following the Colorado floods of 2013, we implemented a study to determine whether changes in the landscape could be detected from remotely sensed satellite imagery. We concluded that flooding effects, in terms of infrastructure damage and water movement patterns, could indeed be seen in these images.

We also conducted an investigation to examine the characteristics of pavement photographs. Photographs of good and poor pavement were collected and digitally analyzed. There is a clear difference between the statistical distributions of the pixel brightness values for the good and poor pavement photographs. The spatial resolution of these photographs was then downsampled to the resolution of WorldView-2's panchromatic band and the images were corrupted with noise. The same type of analysis was performed on these images and similar results were obtained. These results suggest that pavement surface quality can be automatically obtained from images alone, that is, without in situ surveillance methods.

We continued the experiment which involved texture filtering of satellite images to assess road surface quality. Previously, we only observed extreme cases of "good" and "poor" pavement condition. However, this time we observed the intermediate "fair" condition as well. Our results suggest that as highway pavement degrades, its appearance becomes brighter and more varied. Since these characteristics are detectable in satellite imagery, we believe that a pavement condition classification scheme can be developed.

The results of these analyses are presented in this report.

I — TECHNICAL STATUS

Part 1: Road Disruption in the Colorado Flood from Satellite Imagery

The 2013 Colorado floods were a natural disaster occurring in the U.S. state of Colorado. During the week starting on September 8, a slow-moving cold front stalled over Colorado, clashing with warm humid monsoonal air from the south. This resulted in heavy rain and catastrophic flooding along Colorado's Front Range from Colorado Springs north to Fort Collins. The situation intensified on September 11 and 12. Boulder County was worst hit, with 9.08 inches (231 mm) recorded September 12 and up to 17 inches (430 mm) of rain recorded by September 15, which is comparable to Boulder County's average annual precipitation of 20.7 inches (525 mm).

At least eight deaths have been reported by the Colorado Office of Emergency Management, with two more missing and presumed dead and hundreds remaining unaccounted for. More than 11,000 have been evacuated. The town of Lyons in Boulder County was isolated by the flooding of St. Vrain Creek. Several earth dams along the Front Range burst or were over-topped. On September 12, Boulder Creek was reported to have exceeded a flow rate of 5,000 cubic feet (140 m^3) of water per second. Boulder Creek regularly flows around 150–200 cubic feet (4.2–5.7 m^3) per second. This caused serious damage to buildings along the creek and the creek path such as Boulder High School. As of late September 13, according to the Office of Emergency Management, there were 172 people unaccounted for and at least three dead in flood areas of Boulder County. By September 14, the death toll had reached five and more than 500 were unaccounted for, but not necessarily considered missing. The flood resulted in many bridges and road sections being washed out (Fig. 1) and entire towns being stranded due to lack of road access.

Fig. 1: A bridge collapse on a business access road at Highway 287 and Dillon Road In Lafayette causes three cars to fall into the creek on Sept. 13.

High-resolution (~2 m) satellite images clearly show these disruptions when comparing an image before the flood (Fig. 2) and after the flood (Fig. 3).

Fig. 2: Before the flood

Fig. 3: After the flood

It can clearly be seen here that the highway in the middle of the image was washed out in the lower half by the flood. Water has completely erased the road surface and the reflectivity now merely indicates the presence of water.

Fig. 4: Before the flood

Fig. 5: After the flood

In Figs. 4 and 5, one can see the destruction of a highway bridge as the river rerouted its path and flooded many regions downstream of the bridge. This was one of the more destructive effects of the flood which resulted in permanent rerouting of the river and the need for new bridges to be built or an effort be made to return the river to its original course. It is this type of destruction that led to scenes like that in Fig. 1. Again, these two high-resolution satellite images clearly depict the damage caused and suggest solutions that need to be considered.

A change detection study of two satellite images from this period demonstrated the very marked changes from non-flooded (Fig. 6) to flooded conditions (Fig. 7).
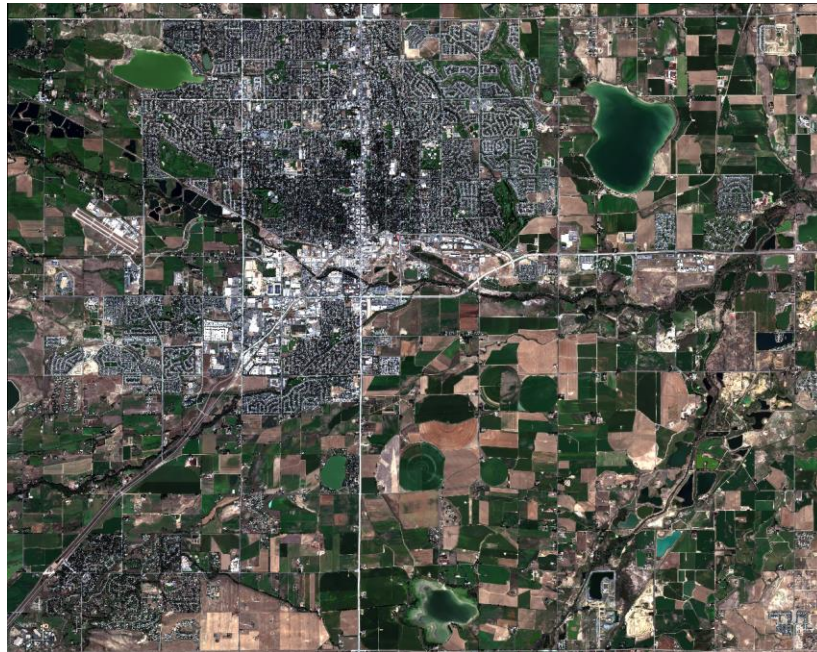
Fig. 6: Before the flood

Fig. 7: After the flood

These images cover part of the western side of Longmont, Colorado where east-west Colorado State Highway 119 intersects with north-south U.S. Route 287.

Due to the computational complexity of classifying these large high-resolution images, smaller image segments were selected and analyzed for surface changes due to flooding. One such image segment is shown in Fig. 8 before the flood and in Fig. 9 after the flood.

Fig. 8: Before the flood

Fig. 9: After the flood

Here, flooding is again readily apparent in the muddy water that now connects the two central lakes and has expanded their boundaries. The other lake in right hand side of the image has also changed to muddy water. Using Change Vector Analysis (CVA), the changes between these last two images were classified. In this algorithm, the changes are resolved in 2D vector space to normalize the changes. Using image reflectances to compensate for solar illumination, the CVA analysis was carried out between Fig. 8 and Fig. 9. The results are shown here in Fig.

10, where changed areas are marked by specific colors. The legend to these changes is also given in the figure. In most cases, the changes are to water but in some soil areas, the immediate response to being soaked was a rapid response to vegetation. This is typical of Colorado where the generally dry soil transitions quickly to vegetation when water is applied particularly in large amounts.
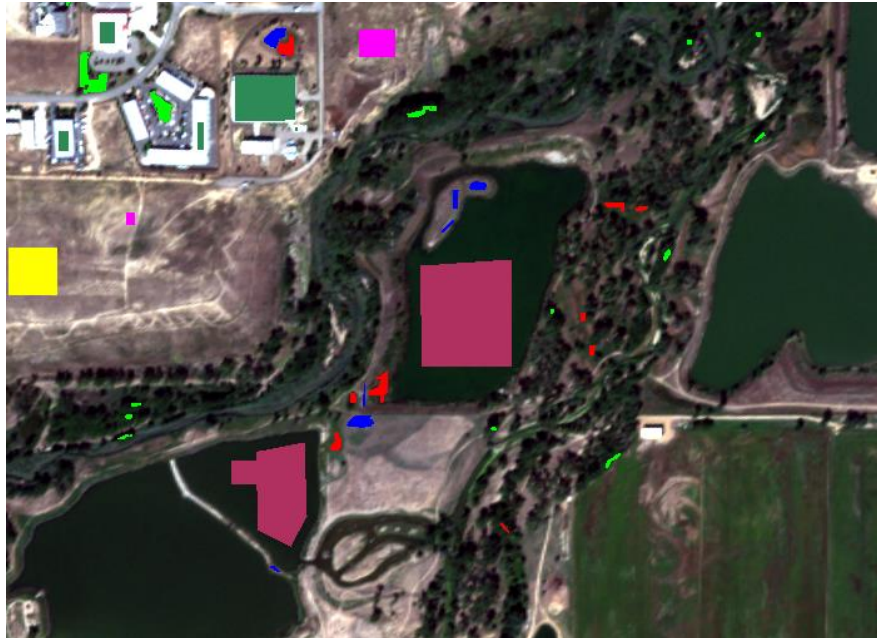
Red: veg2wat
Blue: soil2wat
Green: veg2veg
Magenta: soil2soil
Cyan: wat2wat
Sea green: roof2roof
Yellow: asph2asph

Fig. 10: The "before" satellite image with colors marking the "after" changes

There is, however, asphalt (parking lot) that does not change and remains asphalt.

Summary of Part 1

Satellite imagery clearly shows the destruction of road infrastructure (roadbeds, bridges, unpaved roads) that are caused by episodic flooding such as what occurred in the Boulder County flood of September 2013. It can be used to help guide recovery efforts by clearly showing surface conditions after a flood has occurred. Satellite images can also help us to understand the surface condition changes post flood as the flood waters recede. Automated techniques can be employed to quantify surface changes and guide the use of these satellite images for both planning, evaluation, disaster management and recovery efforts.

Part 2: Statistical Analysis of Pavement Imagery

As an extension of our study of road surface imagery, we began a parallel study to better understand the ability of a satellite image to detect changes in road surface conditions in the presence of noise. To evaluate this aspect of our image analysis, photographs of parking lots differing in pavement surface quality were collected with a mobile phone digital camera. These photographs were then downsampled to a lower resolution consistent with the satellite image resolution and corrupted with noise consistent with estimates of the noise in the satellite imagery. In this way, we hope to simulate imagery from DigitalGlobe's WorldView-2 spacecraft. The statistical characteristics of both the original mobile phone photographs and the simulated

satellite images were computed and examined. The purpose of this investigation was to reinforce the idea that information regarding pavement surface quality could indeed be obtained through satellite remote sensing.

Image Data Collection

Photographs of two different parking lots were collected for this study. The first parking lot was located in the University of Colorado – Boulder campus south of Colorado Avenue between the Duane Physics & Astrophysics and Benson Earth Sciences buildings. The pavement of this lot had a dark and smooth appearance with no signs of wear and tear. If it were surveyed by CDOT, it would likely receive a condition rating of "good". The second parking lot was located in the East Aurora neighborhood of Boulder on the northwest corner of 29th Street and Bixby Lane directly north of the Spanish Towers apartment building. The pavement of this lot had a speckled and rough appearance. It was also marked with numerous distresses such as cracking, potholes, and worn out sealant. If it were surveyed by CDOT, it would likely receive a condition rating of "poor". The stark contrast between these two parking lots would make for an interesting analysis.

It was previously believed that direct sunlight on cloudless days was necessary to illuminate the pavement properly. Photographs of these parking lots were thus initially collected on sunny days. However, preliminary analysis revealed that direct sunlight brought about uneven illumination of the pavement. The photographs were reshot on cloudy days and illumination of the pavement became more uniform. Therefore, pictures from cloudy days were used in this study instead.

Pavement Images

The two parking lot images used in this study are shown here in Fig. 11.
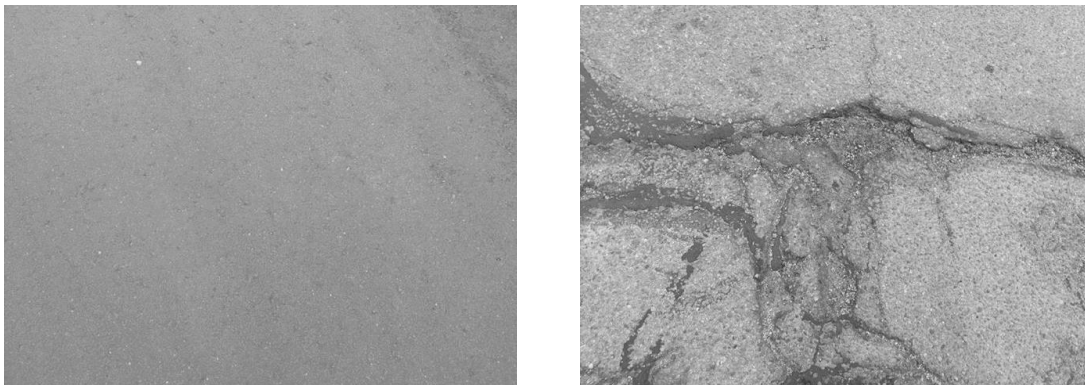
Fig. 11: Parking lot images, good pavement on the left and poor pavement on the right

Notice the relatively smooth appearance of the good pavement compared to the speckled and distressed appearance of the poor pavement.

Satellite Image Synthesis

The greyscale images of the parking lot pavement were manipulated to imitate imagery from WV-2. The first step was to reduce their spatial resolution to match the ~50 cm resolution of WV-2. The spatial resolution of the mobile phone photographs was determined to be 500 times greater than that of the satellite. Thus, the parking lot images were downsampled by this factor,

resulting in new greyscale images with a size of 7×5 pixels.

The next step was to add noise to these 7×5 images representative of the noise characteristics of the WV-2 sensor. The WV-2 images provided by DigitalGlobe have 11-bit digital number (DN) values. Brighter landscapes have higher DN values and darker landscapes have lower DN values. Experiments conducted by scientists at DigitalGlobe have determined that the noise variance associated with DN is linearly proportional to DN itself. To measure the sensor's noise, the WV-2 radiometer was pointed at a cloudless scene of free space between the Moon and the Earth. The DN values in the two-dimensional image of this scene are constant in the horizontal direction but continuously varying in the vertical direction. Sample image chips were collected along the horizontal direction at different vertical positions. The DN variances and DN means of each chip were obtained and plotted against each other. The results of one trial are shown in Fig. 12 below.
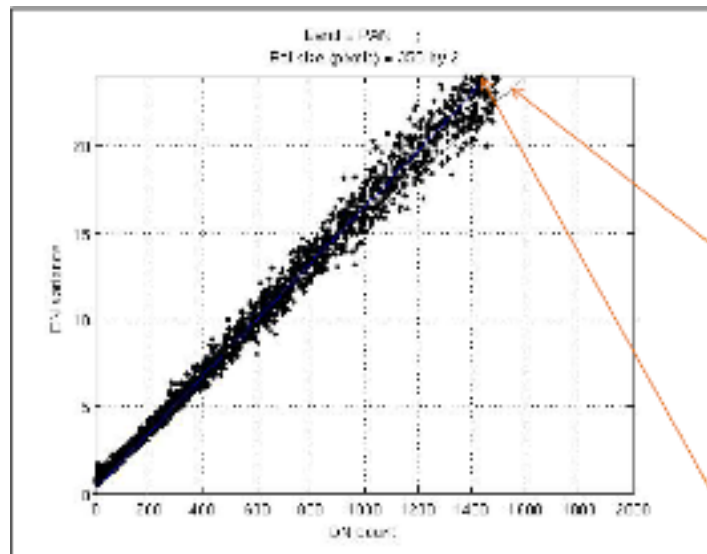
Fig. 12: WV-2 DN Variance vs. DN Count.

The 7×5 greyscale images of the parking lots were corrupted by artificial noise equivalent to that of the WV-2 sensor. The "clean" 8-bit greyscale values in the pixels of a given image were multiplied by 2^3 to simulate 11-bit DNs. The noise variances were calculated for each pixel. A Gaussian random number generator was used to produce noise values at every pixel with zero mean and a standard deviation of the noise distribution. The resulting noise values were added to the mock DNs to create "noisy" DNs. The "noisy" DNs were divided by 2^3 to simulate corrupted 8-bit greyscale values, which will henceforth be referred to as DN values. The 8-bit greyscale images constructed from these artificially corrupted pixels finally represent the desired mock WV-2 imagery.

Occurrence-Based Texture Filtering

We used occurrence-based texture filters to bring out the character of each image. In such a procedure, a rectangular subsection of an image, called the sliding window, is selected and passed over the entire image. The texture statistics are computed in each sliding window, which have odd dimensions to ensure that the resulting texture statistic can be located at the central pixel. Texture statistics are calculated as the sliding window is passed over the image until all pixel locations have a texture value. The occurrence-based texture parameters are:

Data range = $\max I(i,j) - \min I(i,j)$

Mean = $\mu = \sum_{ij} I(i,j)p(i,j)$

Variance = $\sigma^2 = E[(I(i,j) - \mu)^2]$

Entropy = $-\sum_{ij} p(i,j) \ln p((i,j)$

Skewness = $E[((I(i,j) - \mu)/\sigma^3]$

Here, i and j represent the horizontal and vertical indices of the image pixels contained within the sliding window. The term I(i, j) is the image brightness at the pixel location (i, j) and the term p(i, j) is the probability mass function of the I(i, j) value.

Data range gives an indicator of how far apart the lowest and highest brightness values of the window are. The mean is the average brightness of the window while the variance indicates how far the majority of the values lie with respect to the mean. Entropy is a measure of the statistical randomness in the window. Skewness indicates the degree of asymmetry of the spread in the probability density function.

Application to the Full Resolution Images

These texture filters were initially applied to the full digital images shown here in Fig. 11. Looking first at the digital numbers before applying the texture filters, we find that even here there are some marked differences between the good and poor parking lot surfaces.
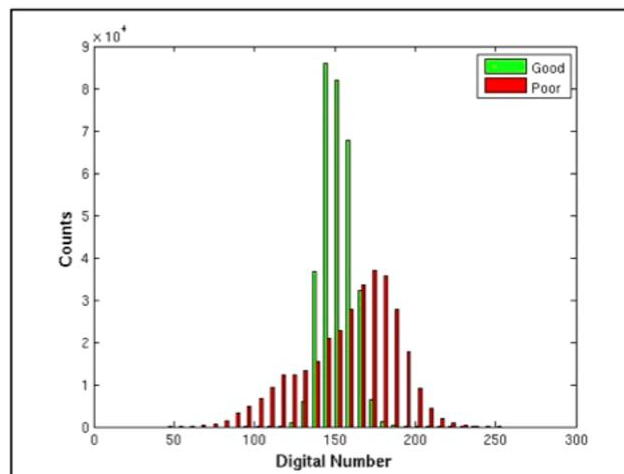
Fig. 13: Histogram of DN values for both surfaces.

Note the dramatic difference between the poor histogram with its wide spread in values versus the good histogram which has a much more limited range of values.

The histograms from the mean filter (not shown) look very similar to the DN histograms. The

good mean histogram also has a narrow distribution and the poor mean histogram also has a wide distribution. The variance (not shown) reveals a very high histogram for the good image at the lower values suggesting a relatively uniform response for the smallest scales. The poor pavement surface has a slightly wider range but also falls off exponentially as the bins get higher. Turning to entropy, we find in Fig. 14 that the good pixels overall have lower values than the poor pixels, which stand out at the highest bins. This is again consistent with the poor surfaces linking to high entropies and the good surfaces corresponding to low entropies.
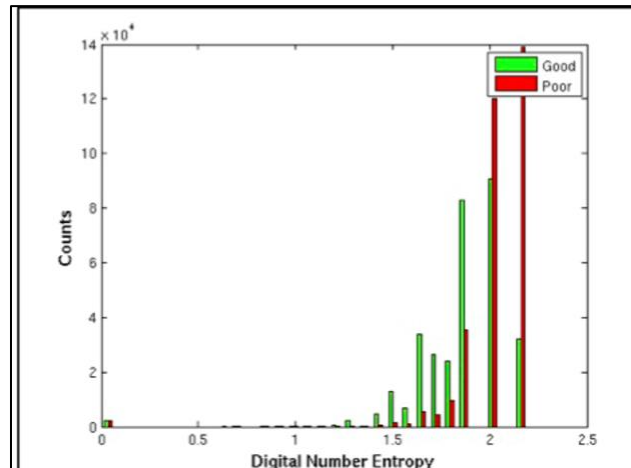
Fig. 14: Image entropy Histogram

The means and standard deviations of all the histograms are presented here in Table 1 for the original resolution images.

	Good Mean	Good STD	Poor Mean	Poor STD
Digital Number	152.3	9.8	159.7	29.0
Data Range	16.1	8.5	42.8	20.8
Mean	151.3	15.1	158.6	28.2
Variance	30.6	42.3	222.3	241.0
Entropy	1.9	0.3	2.1	0.2

Table 1: Image Histogram Properties (full resolution)

Synthetic Satellite Image Analysis

The next step was to follow the procedure outlined above to downsample the digital images to the satellite resolution and then add noise representative of the WV-2 satellite images. The downsampled images are presented here in Fig. 15 again with the good image on the left and the poor surface image on the right.
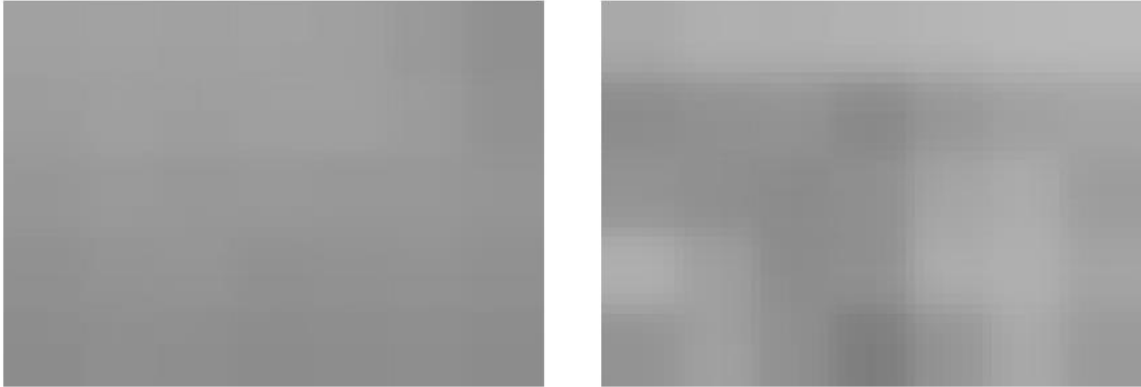
Fig. 15: Synthetic WV2 images of good pavement (left) and poor pavement (right)

The subsampled images are only 7X5 pixels but they do match the WV2 50 cm resolution. What results are clearly blurred versions of the originals in Fig. 11 but as the analysis will show they retain a lot of the basic texture information of the original images. Recall also that noise has been added to each image that will distort the final images even more.

To compute the occurrence-based texture filters we had to move to a 3X3 sliding window, which results in only 15 pixels for the computation of the texture filters. This is far too few to compute histograms as we did earlier but fortunately there were 24 images per surface condition rather than a single high-resolution image. Thus, we can use these repeat images to compute the histograms.

The DN histogram is presented here in Fig. 16 using the same labels as in the previous histograms.
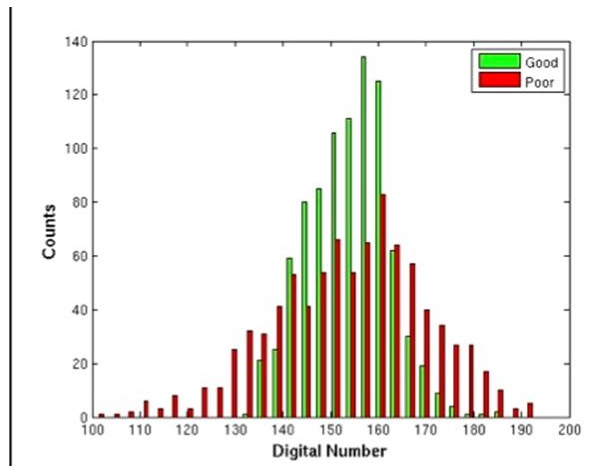
Fig. 16: Histograms of synthetic satellite image DNs.

While the spread of the good histogram is much greater than that in Fig. 13, it is again located in the center of the DN range at numbers very close to those in Fig. 13. Qualitatively, the Fig. 13 and 16 are very similar.

Once again, the mean histograms of the lower resolution histograms (not shown) look very similar to the histograms of the DN values, like what was seen in the higher resolution example. The variance (not shown) is also very similar between these two different resolutions. Finally, the entropy histograms of Fig. 17 look similar to the same entropy plot for the high-resolution images in Fig. 14. Again, the poor pavement histogram has very high peaks at the largest bins while the good surface histogram peaks spread out over a much larger range and have overall lower values.
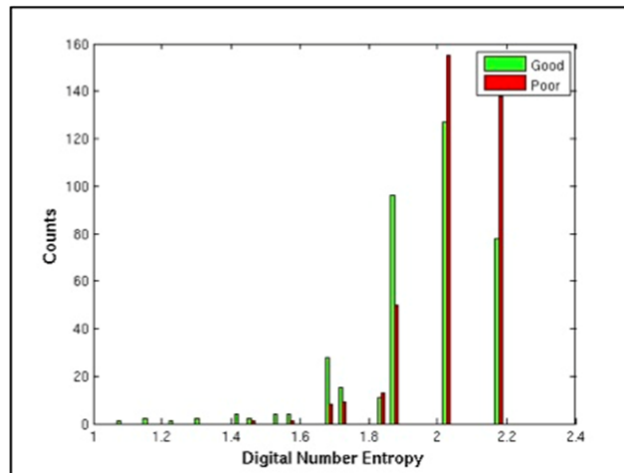
Fig. 17: Histograms of synthetic image entropies.

A summary of the means and standard deviations are presented here in Table 2.

	Good Mean	Good STD	Poor Mean	Poor STD
Data Range	14.2	4.9	34.9	12.3
Mean	154.1	5.3	152.2	9.3
Variance	23.6	16.0	148.8	104.4
Entropy	2.0	0.2	2.1	0.1

Table 2: Image histogram properties for synthetic WV-2 images

It is encouraging that the histograms of both the high-resolution images and the subsampled plus noise synthetic WV-2 satellite images behave similarly. This result suggests that indeed it should be possible to clearly discriminate between poor and good pavement surfaces using simple texture analyses on satellite imagery.

Summary and Conclusions for Part 2

The ultimate goal of this investigation was to demonstrate that pavement surface quality could be assessed from images of the pavement itself, even at the spatial resolution of WV-2 satellite images. Although it may seem obvious when approached qualitatively, the results of this study serve as evidence that the concept can be implemented quantitatively. There are clear differences in the way that the statistical information of the good and poor pavement photographs is distributed. These statistics verify that good pavement appears uniform when compared to poor pavement, which appears more varied. These differences are not only present at the comparatively high-resolution photographs, but also at the lower resolution and noisier synthetic satellite images.

Future Work in this Area

If this investigation were to hypothetically continue, there is some room for improvement. One possibility would be to survey a wider variety of pavement conditions. For example, instead of just examining extremely good and extremely poor pavement, more intermediate quality pavement could be examined. If the statistics of this fair quality lie in between that of the good and poor, then that would strengthen the results of this study even further. Also, some better photograph capturing techniques could be used. Although the mobile phone camera has been quite reliable, it was difficult to keep steadily pointed towards nadir at a constant height. And since it was only held a few feet above the ground, its field of view was not very wide. In order to match the resolution of the WorldView-2 satellite sensor, the pictures needed to be scaled down by a large factor, which caused a drastic reduction in pixel samples. Perhaps an apparatus could be built to hold the camera steady at a higher height in future surveys to mitigate these issues. Nonetheless, this investigation has been fruitful overall and the results will undoubtedly aid us as we continue to assess the feasibility of using remote sensing techniques to study pavement surface quality.

Part 3: Using high-resolution satellite data to assess road surface conditions

Most of the first year of this project was wasted in trying to find direct relationships between the satellite image data and the in situ measured parameters of International Roughness Index (IRI), rutting and cracking (fatigue, etc.). We were not able to find any statistically significant relationships with these 3 variables. We later learned several things:

a. We learned that there are serious statistical limitations to the in situ data that contributed to our inability of using the satellite DN values to properly estimate any of these parameters. We were eventually able to use visual analysis of the satellite imagery to come up with an estimate of cracking only.

b. We also learned that the in situ data are generally processed by manually leading to a greater noise level in terms of both mislocation and in the estimate of the value.

c. Finally we learned that these in situ parameters are all combined to come up with a rating of Good, Fair, and Poor (CDOT has 2 levels of Poor) road surface conditions and that the decisions to repave a road surface are made based on these broad categories and not on a specific value of IRI, rutting or cracking.

We decided to focus our efforts on using the high-resolution satellite data to estimate the Good, Fair, and Poor conditions of the road surfaces. We primarily used CDOT highways since they assess their road condition every year to update their ratings and make repaving decisions. We decided that the best way to take full advantage of the high-resolution satellite imagery was to carry out a texture analysis of the satellite images to see if we can find correspondence with the Good, Fair and Poor conditions of the CDOT highways.

In Quarterly Progress Report #4, we presented the results of a study in which we applied texture filters to satellite images of just good and poor highways. We extended this analysis to see if it would be possible to estimate fair road surface conditions from the WV-2 panchromatic satellite imagery as well. While doing so, we had to recognize that in addition to the pavement properties themselves, there are several other factors, which can affect the digital number

values. They include, but are not limited to, solar incidence angle, satellite viewing angle, and atmospheric phenomena like clouds. To control for these factors, we made sure that all the roads that we examined were part of the same image set. That way, the only variations in the digital numbers would be from just the pavement properties.

The roads that were examined in this study are located around Colorado Springs. They are segments of highway stretches 21B, 115A, and 24A (Fig. 18). They have been rated by CDOT as having conditions of good, fair, and poor respectively. The remotely sensed images were collected by WorldView-2 last year around Thanksgiving. The aforementioned highways are shown below.

Fig. 18: From left to right, 21B, 115A, and 24A

We selected Regions of Interest (ROIs) from these images to study. We were a bit more meticulous than before regarding which parts of the roads were selected. We avoided objects that obviously weren't part of the roads like vehicles and shadows. Another test case that we previously worked on showed that the paint lines throw off the statistics. So by avoiding the paint and other non-road surface image elements only the pavement was looked at. The pictures below show the ROIs laid over the roads (Fig. 19).

Fig. 19: From left to right: 21B, 115A, and 24A ROIs

We extracted the digital numbers contained within the pixels underneath the ROIs. We also applied the occurrence-based texture filters to these images and extracted data from those same pixels. There were about 1600-1800 data points for each road segment, so we just randomly selected 1500 from each segment. We plotted the data from each texture parameter as histogram shown below (Fig 20).

b.

c.

d.

e.
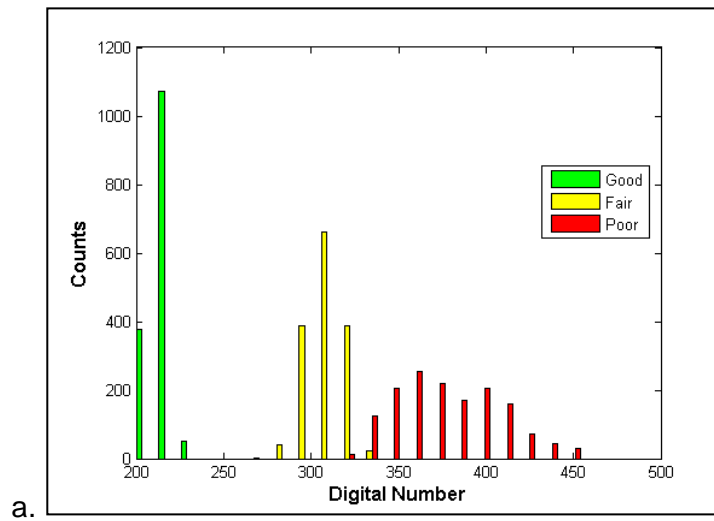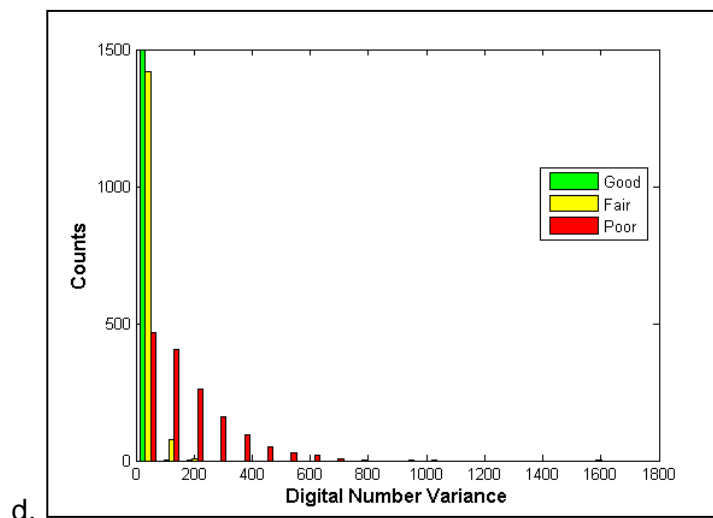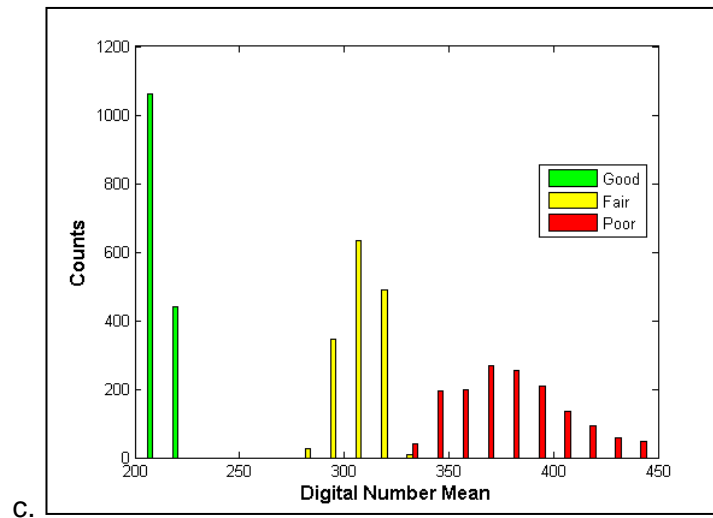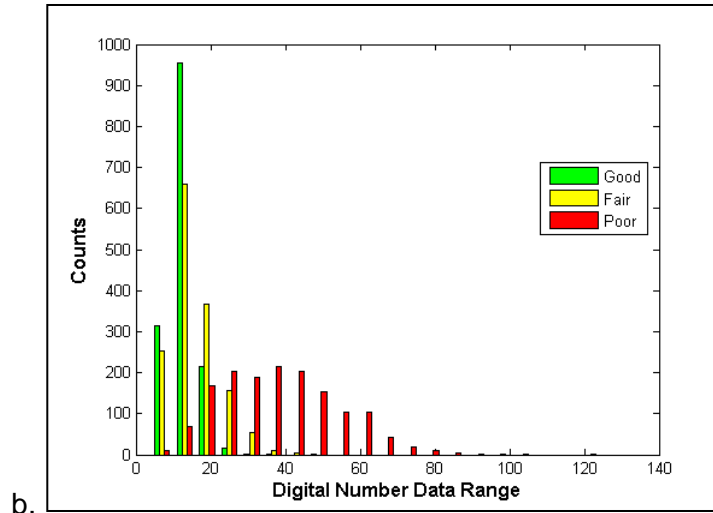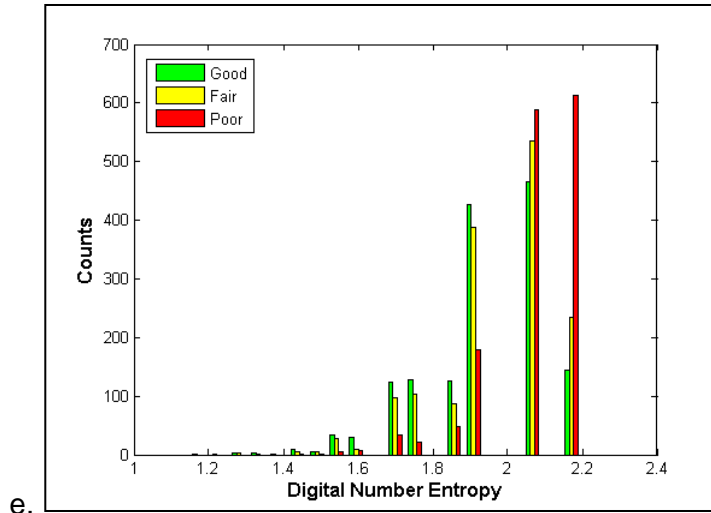
Fig. 20: Histograms of (a) DN, (b) data range, (c) mean, (d) variance, (e) and entropy

The tables below show the means and standard deviations of the histograms above.

	Good	Fair	Poor
DN	214.3	307.7	377.7
DN Data Range	13.3	16.1	38.7
DN Mean	214.5	307.8	378.3
DN Variance	18.7	31.5	174.0
DN Entropy	1.9	2.0	2.1

Table 3: Means of histograms

	Good	Fair	Poor
DN	5.2	10.3	29.5
DN Data Range	3.5	6.2	15.6
DN Mean	3.1	8.8	26.4
DN Variance	10.7	27.6	145.7
DN Entropy	0.2	0.2	0.1

Table 4: Standard Deviations of histograms

Once again, the results suggest that as a road's condition worsens, its appearance becomes more heterogeneous. But these results are even stronger than what we had before. In the previous analyses, we were only comparing good and poor. But here, we have the intermediate fair condition. In every single one of the texture parameters, the fair data lies between the good and the poor, which is what should happen. Hence we believe we should be able to detect and define Good, Fair and Poor road surface conditions based on WV high-resolution satellite imagery. The next step will be to work with CDOT to develop some test cases where the satellite imagery can be used to determine conditions that are then confirmed by in situ sampling and CD field analyses.

Future Plans

The results from this study strongly suggest that the most promising way to determine pavement surface conditions through remote sensing methods is to analyze the texture characteristics of the satellite images. We will continue to improve this technique so that we can understand how the statistics of good, fair, and poor surfaces are distributed. We hope to figure out a way to control for factors such as solar incidence angle, satellite viewing angle, and atmospheric conditions. By doing so, the only elements that contribute to the appearance (i.e. DN values) of the pavement surface in the satellite images would involve the pavement alone.

Because features in the roads such as vehicles, shadows, paint lines, etc. can introduce unwanted variations in the texture filtered images, the regions of interest had to be manually selected in order to avoid them. This is a tedious process that we would like to avoid. We will try to develop a process that can perform this task automatically.

We intend to eventually test out this technique in coordination with CDOT. While CDOT performs its annual surveys, we shall try to assess the pavement condition of several highways through our remote sensing methods. If our results match those of CDOT, then that would be a major sign of success for this project.

II — BUSINESS STATUS

Please see Appendix.

FEDERAL FINANCIAL REPORT
(Follow form instructions)

1. Federal Agency and Organizational Element to Which Report is Submitted Department of Transportation	2. Federal Grant or Other Identifying Number Assigned by Federal Agency (To report multiple grants, use FFR Attachment) RITARS-12-H-CUB	Page 1	of 1 pages

3. Recipient Organization (Name and complete address including Zip code)

THE REGENTS OF THE UNIVERSITY OF COLORADO, 572 UCB,3100 MARINE ST, BOULDER CO 80309

4a. DUNS Number 00-743-1505	4b. EIN 846000555	5. Recipient Account Number or Identifying Number (To report multiple grants, use FFR Attachment) 1549569 & 1549570	6. Report Type ✓ Quarterly ☐ Semi-Annual ☐ Annual ☐ Final	7. Basis of Accounting ✓ Cash ☐ Accrual

8. Project/Grant Period From: (Month, Day, Year) 08/15/2012	To: (Month, Day, Year) 08/14/2014	9. Reporting Period End Date (Month, Day, Year) 12/31/2013

10. Transactions	Cumulative
(Use lines a-c for single or multiple grant reporting)	
Federal Cash (To report multiple grants, also use FFR Attachment):	
a. Cash Receipts	174,694.40
b. Cash Disbursements	207,089.55
c. Cash on Hand (line a minus b)	-32,395.15
(Use lines d-o for single grant reporting)	
Federal Expenditures and Unobligated Balance:	
d. Total Federal funds authorized	509,290.00
e. Federal share of expenditures	207,089.55
f. Federal share of unliquidated obligations	0.00
g. Total Federal share (sum of lines e and f)	207,089.55
h. Unobligated balance of Federal funds (line d minus g)	302,200.45
Recipient Share:	
i. Total recipient share required	509,290.00
j. Recipient share of expenditures	221,266.80
k. Remaining recipient share to be provided (line i minus j)	288,023.20
Program Income:	
l. Total Federal program income earned	0.00
m. Program income expended in accordance with the deduction alternative	0.00
n. Program income expended in accordance with the addition alternative	0.00
o. Unexpended program income (line l minus line m or line n)	0.00

11. Indirect Expense	a. Type	b. Rate	c. Period From	Period To	d. Base	e. Amount Charged	f. Federal Share
	Predetermin	52.50%	8/15/12	12/31/13	121572.15	63825.40	63825.40
		0.00%					
				g. Totals:	121,572.15	63,825.40	63,825.40

12. Remarks: Attach any explanations deemed necessary or information required by Federal sponsoring agency in compliance with governing legislation:
Tuition charges of $21,583.00 is exempt from F & A base. Only first $25K on sub-contract is charged with F&A.

13. Certification: By signing this report, I certify that it is true, complete, and accurate to the best of my knowledge. I am aware that any false, fictitious, or fraudulent information may subject me to criminal, civil, or administrative penalities. (U.S. Code, Title 18, Section 100 1)

a. Typed or Printed Name and Title of Authorized Certifying Official Andy Wang, Grant Accountant	c. Telephone (Area code, number and extension) 303-492-8925
	d. Email address xingji.a.wang@colorado.edu
b. Signature of Authorized Certifying Official Andy Wang Digitally signed by Andy Wang DN: cn=Andy Wang, o=Sponsored Project Accounting, ou=The University of Colorado at Boulder, email=xingji.a.wang@colorado.edu, c=US Date: 2012.05.24 19:08:37 -06'00'	e. Date Report Submitted (Month, Day, Year) 01/09/2014
	14. Agency use only:

Standard Form 425
OMB Approval Number: 0348-0061
Expiration Date: 10/31/2011